HHS Public Access

Author manuscript

AJR Am J Roentgenol. Author manuscript; available in PMC 2020 January 07.

Published in final edited form as:

AJR Am J Roentgenol. 2019 March ; 212(3): 547–553. doi:10.2214/AJR.18.20284.

Noninvasive Multi-parametric CT Staging of HCV-related Liver Fibrosis::

Correlation with the Histopathologic METAVIR Fibrosis Score

Perry J. Pickhardt, **Peter M. Graffy**, **Adnan Said**, **Daniel Jones**, **Brandon Welsh**, **Ryan Zea**, **Meghan G. Lubner**

The University of Wisconsin School of Medicine & Public Health, Madison, WI

Abstract

Purpose: To develop a multi-parametric CT algorithm to stage liver fibrosis in patients with chronic hepatitis C virus (HCV) infection.

Methods: Abdominal CT and laboratory measures in 469 HCV patients (mean age, 50.1 years; 340M/129F) was compared against the histopathologic METAVIR fibrosis reference standard (F0=49, F1=69, F2=102, F3=76, F4=173). From the initial candidate pool, nine CT and two laboratory measures were included in the final assessment (CT-based features: hepatosplenic volumetrics, texture features, liver surface nodularity (LSN) score, and linear CT measurements; lab-based measures: FIB-4 and APRI). Univariate and multivariate logistic regression was performed, with ROC analysis, proportional odds modeling, and probabilities.

Results: ROC-AUC values for the model combining all 11 parameters for discriminating significant fibrosis (≥F2), advanced fibrosis (≥F3), and cirrhosis were 0.928, 0.956, and 0.972, respectively; for all 9 CT-based parameters, these values were 0.905, 0.936, and 0.972, respectively. Using more simplified panels of 2-4 parameters yielded good diagnostic performance; for example, a two-parameter model combining only LSN score with FIB-4 had ROC-AUC values of 0.886, 0.915, and 0.932, for significant fibrosis, advanced fibrosis, and cirrhosis, respectively. LSN score performed best in univariate analysis.

Conclusion: Multi-parametric CT assessment of HCV-related liver fibrosis further improves performance over individual parameters. An abbreviated panel of LSN+FIB-4 approached the diagnostic performance of more exhaustive panels. Results compare favorably with elastography, but this assessment has the advantage of retrospective assessment without planning using pre-existing data.

Corresponding author: Perry J. Pickhardt, MD, Department of Radiology, University of Wisconsin School of Medicine & Public Health, E3/311 Clinical Science Center, 600 Highland Ave., Madison, WI 53792-3252, ppickhardt2@uwhealth.org, phone: 608-263-9028 fax: 608-263-0140.

Disclosures: Dr. Pickhardt: advisor to Bracco; shareholder in Elucent, SHINE, and Cellectar Biosciences

Presented at the 2018 ARRS Annual Meeting

Introduction

Chronic infection with the hepatitis C virus (HCV) can be considered a global health epidemic, as it affects nearly 200 million people worldwide.[1] Progressive hepatic fibrosis leading to cirrhosis may be seen in up to 15–35% of individuals with chronic HCV infection after 25–30 years. Treatment regimens combining newer direct-acting antivirals have resulted in sustained virologic response rates above 90%. However, the high cost of therapy has resulted in the need for accurate staging of hepatic fibrosis related to chronic HCV. Furthermore, even after cure of HCV infection with direct-acting antiviral therapy, the long term change in fibrosis is not clarified. This will require serial re-assessment in these patients to ensure that that there is lack of progression and even regression of advanced fibrosis.

Liver biopsy represents the gold standard for staging hepatic fibrosis. In particular, the METAVIR liver fibrosis scoring system was specifically developed for chronic HCV infection.[2] Use of this metric has been linked to coverage for the newer effective yet expensive drug therapies. Liver biopsy, however, has a number of inherent drawbacks, including invasiveness, cost, and sampling error.[3,4] Accordingly, there has been great interest in validating laboratory and radiologic techniques for noninvasively predicting the degree of liver fibrosis.[4-6] Ultrasound and MR elastography, which estimate liver stiffness as a proxy for fibrosis, are currently in wide clinical use.[7-16] While MR elastography represents a highly effective technique, dedicated equipment is needed that requires prospectively planning, and a number of confounders exist, including ascites, iron overload, and high BMI.[17] As such, the overall technical failure rate may exceed 5% even in expert centers,[15] and may increase to over 15% on 3.0 T MR units.[17]

Abdominal CT is a commonly performed imaging study and is often available for review in patients with chronic liver disease, even if performed for another clinical indication. A number of individual CT-based biomarkers in various mixed and disease-specific patient cohorts have been recently investigated for their ability to estimate liver fibrosis, including measurement of hepatosplenic volumetry,[18,19] liver surface nodularity,[20,21] and liver texture analysis.[22] One advantage of this opportunistic CT approach is the ability to retrospective derive the measurements, with the potential for reducing costs, resource utilization, and avoid the need for prospective planning.

The purpose of this study was to determine if a multi-parametric approach combining various noninvasive CT (and lab) measures can further improve the diagnostic performance for predicting underlying liver fibrosis in patients with chronic HCV infection.

Material and Methods

This single institution retrospective cohort study was HIPAA-compliant and approved by our Health Sciences IRB; the need for additional signed informed consent was waived.

Patient Population

The primary inclusion criteria for eligibility in this study were: 1) HCV positivity via antibody testing (ELISA), which was confirmed with serum HCV RNA PCR, 2) abdominal CT available for review within our PACS system, and 3) liver biopsy within one year of CT (except for cirrhosis exception as described below).

Biopsy was required for all HCV patients in METAVIR F0, F1, F2 and F3 categories, corresponding to no fibrosis (F0), early fibrosis (F1), intermediate fibrosis (F2), and advanced fibrosis (F3).[2] Although biopsy was performed in many F4 (cirrhosis) cases, an exception was deemed necessary for some patients where biopsy was considered to be unnecessary and contraindicated by our hepatologists. These cirrhotic patients without liver biopsy were only included if there were multiple indicators of cirrhosis (chronic end-stage liver disease with or without complications of portal hypertension). Clinical indicators included thrombocytopenia, ascites, and varices, in addition to clear-cut imaging features. In practice, these patients can be confidently diagnosed with cirrhosis based on these parameters without biopsy. This approach has precedent in previous publications.[19-22]

The final patient cohort satisfying the above inclusion criteria consisted of 469 adults (mean age, 50.1 years; 340M, 129F). The METAVIR fibrosis score was F0 in 49 patients, F1 in 69 patients, F2 in 102 patients, F3 in 76 patients, and F4 in 173 patients (86 of these F4 patients underwent liver biopsy)

MDCT Technique

All CT scans were acquired on 16 or 64-detector-row scanners (GE Healthcare). Specific CT protocols were somewhat variable but we focused on the portal venous phase series performed at 120 kV_p for this study; mA settings varied based on patient size and specific study indication. Images were reconstructed using a 5-mm slice thickness at 3-mm intervals using standard filtered back-projection reconstruction with soft tissue algorithm.

CT-based Parameters for Assessing Liver Fibrosis

Prior research informed and substantially limited the choice of included CT parameters, reducing the concern for type-1 multiple-testing error. For example, we chose to only include three texture features and three volumetric measures, in addition to the liver surface nodularity (LSN) score and two simple linear measures. The detailed methodology for some of these measures has been described in previous works,[18-23] but all measures are briefly outlined below and most are demonstrated in Figure 1.

Hepatic and splenic volumetric assessment was performed using a dedicated CT software tool (Liver Analysis application, Philips IntelliSpace Portal), which provides for automated segmentation of the liver and spleen. After initial automated segmentation, organ margins were verified and adjusted if needed with digital brush and eraser tools. Total organ volumes of the liver and spleen were then recorded. Subsequently, Couinaud segments I-III (caudate and left lateral lobe) were isolated from segments IV-VIII. This allows for derivation of the liver segmental volume ratio (LSVR), which has been previously defined as the volume ratio of Couinaud segments I-III to segments IV-VIII.[18,19]

CT texture analysis (CTTA) of the liver utilized a commercially available research software platform (TexRAD Ltd, part of Feedback Plc, Cambridge, UK). Using the software, a region of interest (ROI) was drawn around the liver surface at the level of the porta hepatis, excluding the major hilar vessels (Figure 1). Additional sub-ROIs were drawn approximating Couinaud segments I-III and IV-VIII at this level. Quantification using histogram-based statistical analysis at varying filtration levels (none, fine, medium, and coarse) included various parameters, such as mean gray level intensity (mean), standard deviation (SD), entropy (irregularity), mean of the positive pixels (MPP), skewness (asymmetry), and kurtosis (peakedness). Based on analysis of prior CTTA results,[22] we chose to include only three texture parameters from the IV-VIII sub-ROI for this study (all in portal venous phase): skewness (asymmetry) and kurtosis (peakedness), both with coarse filtration (ssf=6); and mean gray level intensity (mean) with fine filtration (ssf=2).

Liver surface nodularity (LSN) scores were obtained using a validated semi-automated research CT software tool, which is not yet commercially available.[20,24,25] The user digitally "paints" an ROI along the liver surface, which the software automatically detects on the selected slice and adjacent contiguous slices (Figure 1). A series of ≥10 consecutive ROI measurements were made for each case, defaulting along the anterior left lateral liver, and totaling ≥80 cm in length. If the left anterolateral surface was not suitable for LSN scoring, the left medial or right hepatic liver surfaces were utilized. The tool calculates the distance between the detected liver edge and a smoothed polynomial line (spline) that is measured on a pixel-by-pixel basis, and final LSN score is derived.

Two additional linear CT-based measures were added. The periportal space (PPS) is defined by the distance between the anterior wall of the right portal vein and the posterior edge of the medial segment of the left lobe of the liver.[26] This represents a simple measure of fissural widening that accompanies advanced fibrosis and cirrhosis. We also compared the ratio of the left to right portal vein diameters. Similar to the LSVR, this ratio was intended to exploit the regional changes in the liver as fibrosis progresses.

The CT-based measures were made by multiple co-authors, who ranged from 2-20+ years in CT research experience.

Lab-based Parameters for Assessing Liver Fibrosis

We included two well-established serum-based parameters: the APRI and FIB-4 tests were calculated for analysis.[4,5] APRI incorporates liver enzymes (AST) and platelet levels, whereas FIB-4 uses liver enzymes (ALT), platelets, and patient age. Necessary laboratory data were collected, and were required to be within one year of liver biopsy (or CT if no biopsy). Data were available to compute the APRI and FIB-4 measures in 417 patients.

Statistical Analysis

All candidate CT-based and lab-based parameters described above were derived for each patient. Summary statistics (mean, standard deviation, median, and interquartile range) were reported for each parameter according to METAVIR stage of liver fibrosis. Kruskal-Wallis test was used to assess differences for each parameter amongst the discrete F0-F4 sub-cohorts. For all univariate and multivariate performance analyses, emphasis was placed on

the clinically-relevant distinctions of significant hepatic fibrosis (≥F2), advanced hepatic fibrosis (≥F3), and cirrhosis (=F4). Receiver operating characteristic (ROC) curves were obtained for each candidate metric, and areas under the curve (AUC) were calculated, with a DeLong 95% confidence interval. Optimal thresholds were derived to optimize sensitivity and specificity at each fibrosis level. A p-value <0.05 (two-sided) was the criterion for statistical significance. R 3.2.2 (R Core Team 2014) was used for all statistical analyses.

For multivariate analysis, ROC curves were built using a wide variety of combinations ranging from all 11 parameters down to two parameters, based on complementary performance.

Multivariate logistic regression was employed to derive probabilities of being within a given dichotomized category (eg, ≥F3, advanced fibrosis). Logistic regression models the log odds of such an event occurring. Using algebraic techniques, a probability can be recovered from the model in the form of the following equation:

$$p = \frac{e^{(\beta_0 + \beta_1 * x_1 + \cdots + \beta_m * x_m)}}{1 + e^{(\beta_0 + \beta_1 * x_1 + \cdots + \beta_m * x_m)}}$$

The number of evaluable subjects for each parameter is shown in Table S1. Of note, 288 of the 469 patients in this study have been previously reported.[21] This prior article dealt only with the liver surface nodularity CT parameter, whereas the current manuscript reports on a wide variety of parameters, and in a larger cohort.

Results

Univariate Analysis

Summary statistics according to fibrosis category for the eleven individual parameters (nine CT-based and two lab-based) are provided in Table 1 (mean and standard deviations) and Table S2 (median and IQR). All median values for each parameter significantly differed by fibrosis category (p<0.001) except for the LPV/RPV ratio (p=0.352).

Diagnostic univariate performance of each individual parameter for discriminating between stages of liver fibrosis is shown in Table S3, including ROC-AUC, sensitivity, and specificity values. LSN score showed the best univariate performance, and was the only individual parameter to exceed an AUC of 0.900 (0.920 for cirrhosis). Total liver volume and the LPV/RPV ratio were the only two variables not to exceed an AUC of 0.600 for any fibrosis level. Poor performance of total liver volume was expected based on prior research, but this parameter was included as a control of sorts. Most other parameters exceeded 0.800 for at least one fibrosis threshold.

Multivariate Analysis

Table 2 models the ROC-AUC performance for discriminating significant fibrosis (≥F2), advanced fibrosis (≥F3), and cirrhosis for a number of different combinations of parameters. When combining all 11 parameters (9 CT-based and 2 lab-based), ROC-AUC performance

for ≥F2, ≥F3, and ≥F4 (cirrhosis) was 0.928, 0.956, and 0.972, respectively. When the nine CT-based parameters are combined, the corresponding AUC values were 0.905, 0.936, and 0.972, respectively (Figure 2).

As seen in Table 2, more simplified panels consisting of fewer parameters were associated with a modest decline in ROC-AUC values, but relatively good diagnostic performance was observed for some combinations. In particular, a two-parameter model combining only LSN score with FIB-4 showed good complementary performance, with ROC-AUC values of 0.886, 0.915, and 0.932, for significant fibrosis (≥F2), advanced fibrosis (≥F2), and cirrhosis (≥F2), respectively (Figure 2). In general, the model was very good at discriminating advanced fibrosis (F3-F4) from mild (F1) or no (F0) fibrosis, with F2 values being more intermediate between these groups.. Corresponding probability equations were derived. For example, as shown in Figure 3, the probability for advanced fibrosis or cirrhosis (F3-F4) for the LSN + FIB-4 model was:

$$p = \frac{e^{(-6.537 + 1.913 \times LSN + 0.556 \times FIB - 4)}}{1 + e^{(-6.537 + 1.913 \times LSN + 0.556 \times FIB - 4)}}$$

Discussion

Given the revolutionary yet expensive new treatment options now available for chronic HCV, knowledge of the degree of underlying hepatic fibrosis is critical.[1,4] An accurate and accessible method for noninvasive detection, staging, and monitoring of HCV-related fibrosis could have a major clinical impact, and could further reduce the need for liver biopsy.[4,6,16] Obvious drawbacks of liver biopsy include its invasiveness and potential complications, as well as issues of high cost and sampling error. Ultrasound and MR elastography have been extensively studied and are validated for clinical use.[16,27] However, these techniques measure liver stiffness as a proxy for fibrosis, and many confounders exist.[15,28] A number of other potentially useful noninvasive biomarkers based have been proposed and investigated, including both laboratory-based and imaging-based methods.[29]

Recent investigation into a number of intrinsic MDCT imaging biomarkers have shown good correlation with the degree of underlying liver fibrosis.[18-22,29] Such CT features are attractive since they can be derived either prospectively or retrospectively in a planned or opportunistic fashion. Furthermore, because abdominal CT is so commonly performed,[30] there is potential for serial evaluation to look for interval changes.

For the current study, we now take a multi-parametric CT approach and restrict the investigation to only chronic HCV. We excluded many CT parameters prior to embarking on this combined investigation, primarily limiting the focus to the more promising features. We have shown that the diagnostic performance of multi-parametric CT compares favorably with elastography for staging liver fibrosis. In particular, the two-parameter model combining LSN score and FIB-4 showed excellent performance, balancing simplicity and clinical efficacy. As shown by others,[5] we found that FIB-4 outperformed APRI, the other lab-based parameter in our study.

The derivation of probability equations for determining fibrosis suggests a potential way forward in terms of actual clinical implementation. Automation of some of these CT parameters is another potential avenue for future investigation, which would reduce or eliminate the issue of inter-observer variability present in some measures. Finally, it should be noted that many of the CT features we employ could be translated to other cross-sectional imaging techniques, including MR.

We acknowledge limitations to our study. Liver biopsy for staging fibrosis is a fallible reference standard, with issues of inter-observer and sampling error. However, this remains the clinical reference standard for comparison. Direct comparison of our CT-based results with MR (or US) elastography would be of great value, but relatively few patients underwent elastography in addition to liver biopsy. Going forward, we anticipate more patients will undergo MR in lieu of biopsy. Our current results specifically apply to HCV and not other causes of chronic liver disease. However, fibrosis scoring is currently of most clinical relevance in HCV, and more investigational for other etiologies. Finally, this was a single-center study, and multi-center confirmation of our results is warranted. Some multi-institutional work is already underway.

In conclusion, combining key CT-based and lab-based biomarkers of liver fibrosis in a multi-parametric manner further improves their excellent diagnostic performance. Our results for predicting fibrosis stage with CT compares favorably with published results for elastography. Abbreviated panel of 2-4 complementary measures approached the performance of more exhaustive panels, and the simple combination LSN score with FIB-4 may provide an ideal balance of efficacy and ease. Unlike liver biopsy or elastography, these results can be derived retrospectively on routine abdominal CT scans, which may have been obtained for other indications. Furthermore, this approach could be considered for serial assessment of fibrosis in HCV patients given the unknown natural history of fibrosis even after direct-acting antiviral therapy.

Supplementary Material

Refer to Web version on PubMed Central for supplementary material.

Acknowledgments

Funding: This study was supported in part by the Clinical and Translational Science Award (CTSA) program, through the NIH National Center for Advancing Translational Sciences (NCATS), grant UL1TR000427, and by a research grant from Philips Medical

References

1. Thrift AP, El-Serag HB, Kanwal F. Global epidemiology and burden of HCV infection and HCV-related disease. Nature Reviews Gastroenterology & Hepatology 2017;14:122–U68. [PubMed: 27924080]
2. Bedossa P, Poynard T. An algorithm for the grading of activity in chronic hepatitis C. Hepatology 1996;24:289–93. [PubMed: 8690394]
3. Afdhal NH, Nunes D. Evaluation of liver fibrosis: A concise review. Am J Gastroenterol 2004;99:1160–74. [PubMed: 15180741]

4. Martinez SM, Crespo G, Navasa M, Forns X. Noninvasive Assessment of Liver Fibrosis. Hepatology 2011;53:325–35. [PubMed: 21254180]
5. Holmberg SD, Lu M, Rupp LB, et al. Noninvasive Serum Fibrosis Markers for Screening and Staging Chronic Hepatitis C Virus Patients in a Large US Cohort. Clin Infect Dis 2013;57:240–6. [PubMed: 23592832]
6. Nguyen D, Talwalkar JA. Noninvasive Assessment of Liver Fibrosis. Hepatology 2011;53:2107–10. [PubMed: 21547935]
7. Friedrich-Rust M, Nierhoff J, Lupsor M, et al. Performance of Acoustic Radiation Force Impulse imaging for the staging of liver fibrosis: a pooled meta-analysis. Journal of Viral Hepatitis 2012;19:E212–E9. [PubMed: 22239521]
8. Friedrich-Rust M, Ong M-F, Martens S, et al. Performance of transient elastography for the staging of liver fibrosis: A meta-analysis. Gastroenterology 2008;134:960–74. [PubMed: 18395077]
9. Singh S, Venkatesh SK, Wang Z, et al. Diagnostic Performance of Magnetic Resonance Elastography in Staging Liver Fibrosis: A Systematic Review and Meta-analysis of Individual Participant Data. Clinical Gastroenterology and Hepatology 2015;13:440–51. [PubMed: 25305349]
10. Talwalkar JA, Kurtz DM, Schoenleber SJ, West CP, Montori VM. Utrasound-based transient elastography for the detection of hepatic fibrosis: Systematic review and meta-analysis. Clinical Gastroenterology and Hepatology 2007;5:1214–20. [PubMed: 17916549]
11. Wang Q-B, Zhu H, Liu H-L, Zhang B. Performance of magnetic resonance elastography and diffusion-weighted imaging for the staging of hepatic fibrosis: A meta-analysis. Hepatology 2012;56:239–47. [PubMed: 22278368]
12. Castera L, Vergniol J, Foucher J, et al. Prospective comparison of transient elastography, fibrotest, APRI, and liver biopsy for the assessment of fibrosis in chronic hepatitis C. Gastroenterology 2005;128:343–50. [PubMed: 15685546]
13. Foucher J, Chanteloup E, Vergniol J, et al. Diagnosis of cirrhosis by transient elastography (FibroScan): a prospective study. Gut 2006;55:403–8. [PubMed: 16020491]
14. Yin M, Talwalkar JA, Glaser KJ, et al. Assessment of hepatic fibrosis with magnetic resonance elastography. Clinical Gastroenterology and Hepatology 2007;5:1207–13. [PubMed: 17916548]
15. Yin M, Glaser KJ, Talwalkar JA, Chen J, Manduca A, Ehman RL. Hepatic MR Elastography: Clinical Performance in a Series of 1377 Consecutive Examinations. Radiology 2016;278:114–24. [PubMed: 26162026]
16. Tang A, Cloutier G, Szeverenyi NM, Sirlin CB. Ultrasound Elastography and MR Elastography for Assessing Liver Fibrosis: Part 2, Diagnostic Performance, Confounders, and Future Directions. Am J Roentgenol 2015;205:33–40. [PubMed: 25905762]
17. Wagner M, Corcuera-Solano I, Lo G, et al. Technical Failure of MR Elastography Examinations of the Liver: Experience from a Large Single-Center Study. Radiology 2017;284:401–12. [PubMed: 28045604]
18. Furusato Hunt OM, Lubner MG, Ziemlewicz TJ, Munoz Del Rio A, Pickhardt PJ. The Liver Segmental Volume Ratio for Noninvasive Detection of Cirrhosis: Comparison With Established Linear and Volumetric Measures. J Comput Assist Tomogr 2016;40:478–84. [PubMed: 26966951]
19. Pickhardt PJ, Malecki K, Hunt OF, et al. Hepatosplenic volumetric assessment at MDCT for staging liver fibrosis. European Radiology 2017;27:3060–8. [PubMed: 27858212]
20. Pickhardt PJ, Malecki K, Kloke J, Lubner MG. Accuracy of Liver Surface Nodularity Quantification on MDCT as a Noninvasive Biomarker for Staging Hepatic Fibrosis. Am J Roentgenol 2016;207:1194–9. [PubMed: 27575867]
21. Lubner MG, Jones D, Said A, Kloke J, Lee S, Pickhardt PJ. Accuracy of liver surface nodularity quantification on MDCT for staging hepatic fibrosis in patients with hepatitis C virus. Abdominal radiology (New York) 2018.
22. Lubner MG, Malecki K, Kloke J, Ganeshan B, Pickhardt PJ. Texture analysis of the liver at MDCT for assessing hepatic fibrosis. Abdominal Radiology 2017;42:2069–78. [PubMed: 28314916]
23. Lubner MG, Smith AD, Sandrasegaran K, Sahani DV, Pickhardt PJ. CT Texture Analysis: Definitions, Applications, Biologic Correlates, and Challenges. Radiographics 2017;37:1483–U304. [PubMed: 28898189]

24. Smith AD, Branch CR, Zand K, et al. Liver Surface Nodularity Quantification from Routine CT Images as a Biomarker for Detection and Evaluation of Cirrhosis. Radiology 2016:151542.

25. Smith AD, Zand KA, Florez E, et al. Liver Surface Nodularity Score Allows Prediction of Cirrhosis Decompensation and Death. Radiology 2016:160799.

26. Tan KC. Enlargement of the hilar periportal space. Radiology 2008;248:699–700. [PubMed: 18641259]

27. Tang A, Cloutier G, Szeverenyi NM, Sirlin CB. Ultrasound Elastography and MR Elastography for Assessing Liver Fibrosis: Part 1, Principles and Techniques. Am J Roentgenol 2015;205:22–32. [PubMed: 25905647]

28. Wagner M, Corcuera-Solano I, Lo G, et al. Technical Failure of MR Elastography Examinations of the Liver: Experience from a Large Single-Center Study. Radiology 2017:160863.

29. Lubner MG, Pickhardt PJ. MDCT for retrospective, non-invasive staging of liver fibrosis. Gastroenterol Clin North Am (in press).

30. Moreno CC, Hemingway J, Johnson AC, Hughes DR, Mittal PK, Duszak R. Changing Abdominal Imaging Utilization Patterns: Perspectives From Medicare Beneficiaries Over Two Decades. Journal of the American College of Radiology 2016;13:894–903. [PubMed: 27084072]

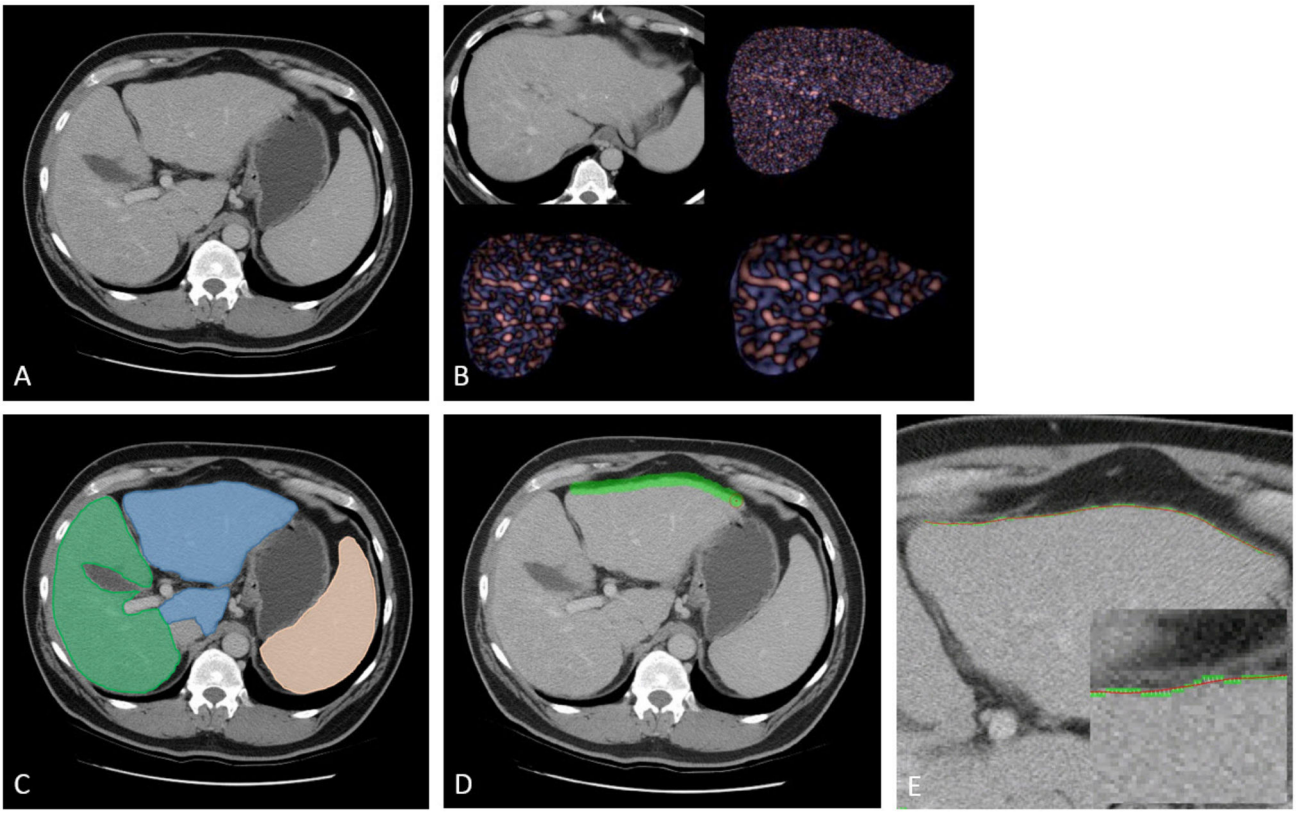

Figure 1. Depiction of CT-based parameters for assessing hepatic fibrosis in 51-year-old with HCV and biopsy-proven F3 fibrosis.

A. Transverse (axial) CT image in portal venous phase shows morphologic changes of advanced fibrosis, including relative enlargement of the left lateral segment, mild surface nodularity, fissural widening, and splenomegaly.

B. Transverse CT image for liver segmentation for texture analysis shows fine filtration (upper right), medium filtration (lower left), and coarse filtration (lower right). Only three texture variables were included in the multi-parametric analysis.

C. Same image from (A) shows cross-sectional representation of hepatosplenic volumetric analysis, including liver segmentation into Couinaud segments I-III (blue) and IV-VIII (green), and splenic segmentation (orange).

D. Same image from (A) now shows process for deriving the liver surface nodularity (LSN) score, which involves tracing along the left anterior liver surface with a broad stroke.

E. Magnified image at same level (including inset image with even more magnification) shows how the LSN tool compares the actual detected liver surface (in green) against a smoothed polynomial line (spline, in red). This is repeated at multiple levels and averaged to derive the final LSN score.

Note: The periportal space and left:right portal vein ratio are not depicted.

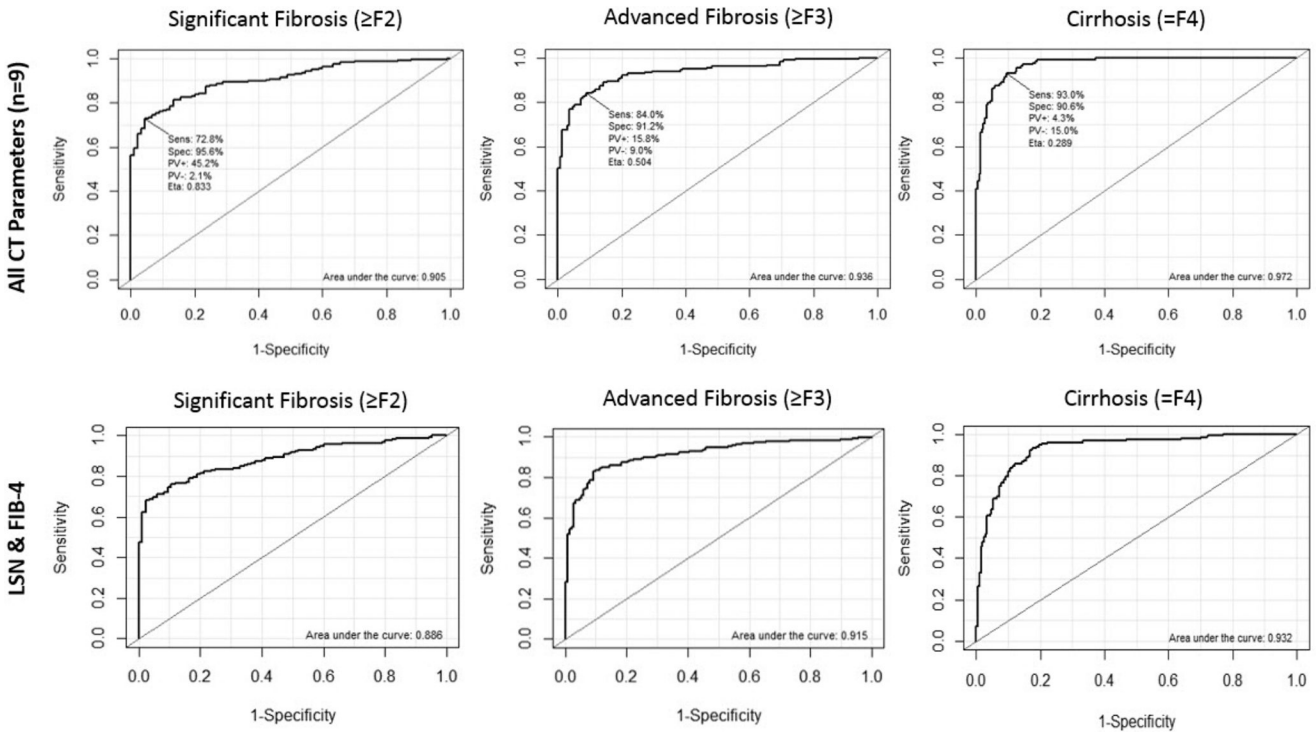

Figure 2. ROC curves from the multi-parametric analysis for all CT input variables and for LSN/FIB-4 combination, according to significant fibrosis (≥F2), advanced fibrosis (≥F3), and cirrhosis (=F4).

Top Row: ROC curves for predicting fibrosis using all 9 CT parameters. AUC values for significant fibrosis, advanced fibrosis, and cirrhosis were 0.905, 0.936, and 0.972, respectively.

Bottom Row: ROC AUC values for the limited combination of LSN score and FIB-4 were 0.886, 0.915, and 0.932, respectively. Only mild drop off in performance is seen, despite using only two complementary parameters (one CT value and one lab value).

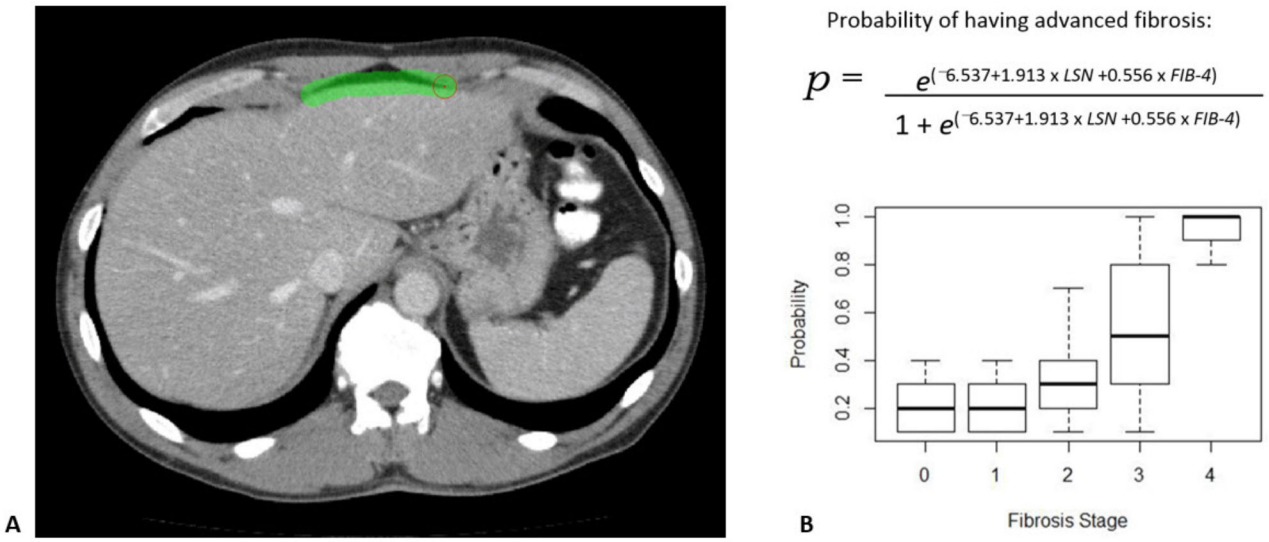

Figure 3. Example case using the simplified LSN score + FIB-4 model: 52-year-old man with biopsy proven F3 fibrosis from chronic HCV

A. CT image in portal venous phase shows LSN score in process. The final LSN score was 2.79. FIB-4 in this patient was 8.15

B. The probability equation for having advanced fibrosis is shown. When plugging in the values for this patient, the probability is 1.0, indicating the patient almost certainly will have advanced fibrosis or cirrhosis. Boxplots of probabilities is shown for the entire cohort.

Table 1.

Mean Values (SD) for CT and Lab Parameters according to Fibrosis Stage

CT (and Lab) Parameters*	Pathologic Fibrosis Stage (METAVIR)				
	F0	F1	F2	F3	F4
LSVR	0.25 (0.08)	0.25 (0.10)	0.28 (0.10)	0.34 (0.12)	0.48 (0.24)
Liver Volume	1676 (359)	1670 (336)	1819 (401)	1974 (476)	1760 (632)
Splenic Volume	278 (138)	285 (134)	329 (187)	474 (375)	782 (451)
LSN Score	2.30 (0.25)	2.31 (0.32)	2.51 (0.46)	2.75 (0.57)	3.85 (1.00)
Periportal Space	6.08 (3.6)	6.41 (3.2)	7.52 (4.3)	7.71 (3.75)	10.13 (4.3)
LPV/RPV Ratio	0.89 (0.14)	0.91 (0.16)	0.91 (0.19)	0.90 (0.16)	0.96 (0.24)
Texture ($Mean_{PV2}$)	0.14 (0.14)	0.28 (0.36)	0.30 (0.29)	0.38 (0.28)	0.89 (0.66)
Texture ($Skew_{PV6}$)	1.55 (0.94)	1.88 (0.74)	1.73 (0.85)	1.68 (0.96)	1.31 (1.01)
Texture (KurtPV6)	1.55 (0.94)	5.17 (5.40)	4.81 (5.58)	5.60 (6.36)	1.82 (2.24)
APRI (Lab)	0.64 (0.6)	0.99 (1.9)	0.94 (1.3)	1.76 (3.5)	4.70 (10.1)
FIB-4 (Lab)	1.20 (0.8)	1.82 (2.2)	2.19 (2.1)	3.87 (6.23)	9.80 (12.6)

*See text for details on parameter description

Table 2.

ROC AUC Values for Multi-parametric Combinations

Parameter Combination*	METAVIR Fibrosis Threshold		
	Significant (≥F2)	Advanced (≥F3)	Cirrhosis (=F4)
All CT + Lab features (11)	0.928	0.956	0.972
All CT features (9)	0.905	0.936	0.972
FIB-4 + APRI (2)	0.843	0.866	0.899
LSN + LSVR + PPS + $Tex_{MeanPV2}$ (4)	0.886	0.923	0.966
LSN + LSVR + PPS (3)	0.879	0.912	0.954
LSN + Spleen + PPS (3)	0.856	0.897	0.938
LSN + Spleen + PPS + FIB-4 (4)	0.892	0.923	0.943
LSN + Spleen + FIB-4 (3)	0.885	0.921	0.940
LSN + Spleen (2)	0.833	0.894	0.937
LSN + FIB-4 (2)	0.886	0.915	0.932
LSN (1)	0.825	0.872	0.920
FIB-4 (1)	0.838	0.857	0.894

*Number in parentheses refer to number of parameters for the given model